Feature paper

Article type: ((**Feature Paper**))

Stabilized dye – pigment formulations with platy and tubule nanoclays

Dr. Bàrbara Micó-Vicent, Prof. Francisco M. Martínez-Verdú, Dr. Andrei Novikov, Dr. Anna Stavitskaya, Prof. Vladimir Vinokurov*, Dr. Elvira Rozhina, Prof. Rawil Fakhrullin*, Dr. Raghuvara Yendluri, Prof. Yuri Lvov**

Dr. B. Micó-Vicent,

Dept. of Applied Statistics, Operational Research, and Quality, Universitat Politècnica de València (Campus d'Alcoi), Spain (Alicante) CP 03801 and University of Alicante, Carretera San Vicente del Raspeig s/n (03690) San Vicente del Raspeig, Spain E-mail: barbara.mico@ua.es

Prof. F.M. Martínez-Verdú,

University of Alicante. Carretera San Vicente del Raspeig s/n (03690) San Vicente del Raspeig (Alicante), Spain E-mail: verdu@ua.es

Dr. A. Novikov,

Addres: I.Gubkin Russian State University of Oil & Gas. 65 Leninsky Prospekt, Moscow, 119991, Russia E-mail: novikov.a@gubkin.ru

Dr. A. Stavitskaya,

Addres: I.Gubkin Russian State University of Oil & Gas. 65 Leninsky Prospekt, Moscow, 119991, Russia E-mail: stavitsko@mail.ru

Prof. V. Vinokurov,

Addres: I.Gubkin Russian State University of Oil & Gas. 65 Leninsky Prospekt, Moscow, 119991, Russia E-mail: vladimir@vinokurov.me

Dr. E. Rozhina,

Address: Department of Microbiology, Institute of Fundamental Medicine and Biology, Kazan Federal University, Kazan, Tatarstan, 420000, Russia E-mail: rozhinaelvira@gmail.com

Prof. R. Fakhrullin,

Address: Department of Microbiology, Institute of Fundamental Medicine and Biology, Kazan Federal University, Tatarstan, 420000, Russia E-mail: kazanbio@gmail.com

Dr. R. Yendluri,

Address: Institute for Micromanufacturing, Louisiana Tech University, 911 Hergot Ave., Ruston, LA 71272 E-mail: rby002@latech.edu

Prof. Y. Lvov.

Address: Institute for Micromanufacturing, Louisiana Tech University, 911 Hergot Ave., Ruston, LA 71272 E-mail: ylvov@latech.edu

Keywords: natual dyes, nanoclays, hybrid pigments, quantum dots

Abstract

The alumosilicate materials of different morphologies such as platy and tubule nanoclays may serve as an efficient protective encasing for the colored organic substances and nanoparticles. The adsorption of dyes onto the nanoclays increases their stability against the thermal, oxidative, and acid-base induced decomposition. Natural organic dyes form stable composites with nanoclays, thus allowing for "green" technology in production of industrial nanopigments. In the presence of high surface area alumosilicate materials, the semiconductor nanoparticles known as quantum dots are stabilized against agglomeration during their colloid synthesis resulting in safe colors. The highly dispersed nanoclays such as tubule halloysite can be employed as biocompatible carriers of quantum dots for the dual labeling of living human cells – both for dark-field and fluorescence imaging. Therefore, complexation of dyes with nanoclays allows for new stable and inexpensive color formulations.

1. Introduction

Inorganic compounds have accounted for over 90 % of the world pigments production. However, the heavy metal content of most inorganic pigments restricts their applications[1]. Natural colorants may substitute synthetic dyes or pigment products. Natural dyes are generally less toxic, biocompatible, more biodegradable, and their production is environmentally friendly[2]. However, currently they have no major industrial applications because of low stability and fast decomposition. Natural organic dyes lose their properties under UV-Vis radiation, at high temperatures, in presence of oxidants, and in wet basic or acidic environment. The other disadvantage of natural dyes is their limited color gamut.

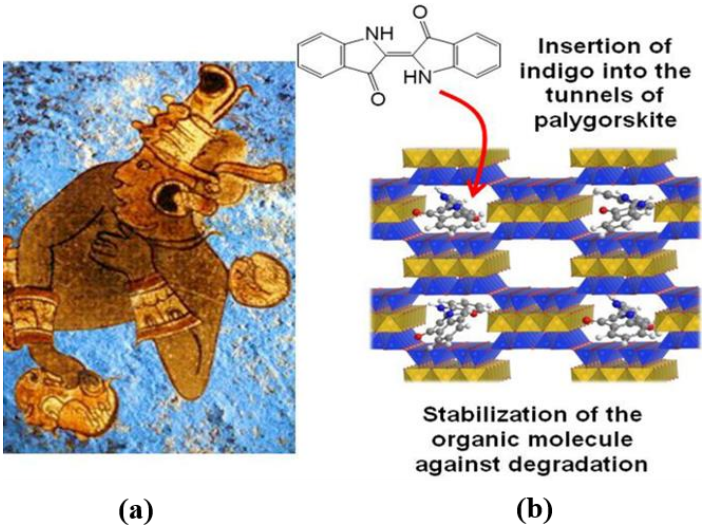

Figure 1. a) An art example for 12th centuary Maya blue indigo color preservation [reproduced with permission https://commons.wikimedia.org/wiki/File:Azulm6.jpg], b) palygorskite – natural indigo interaction scheme

Different alternatives have been sought after for the stabilization of natural dyes. For instance, biomordants from tannin extracts obtained from pomegranate peels were used to improve the natural dyes[3]. One of the most spectacular examples is the ancient Maya technique on the stabilization of indigo 2,2'-Bis(2,3-dihydro-3-oxoindolyliden) in mixture with palygorskite clay, which preserved bright blue color for over 800 years (Figure 1). In this nanocomposite, the dye molecules were placed into 0.64 nm wide tunnels in the clay fibers[4].

The most prominent approach for organic and especially natural dyes protection is their intercalation into inorganic clays, thus having complete operations with "green" natural materials. Abundant bulk clays have to be exfoliated for this purpose, converting to nanomaterials either of lamellar structure with alumo or magnesium/silicate sheets (like kaolin, montmorillonite, bentonite and hydrotalcite) or tubule and fiber structures (halloysite, imogolite, sepiolite and palygorskite), Figure 2.

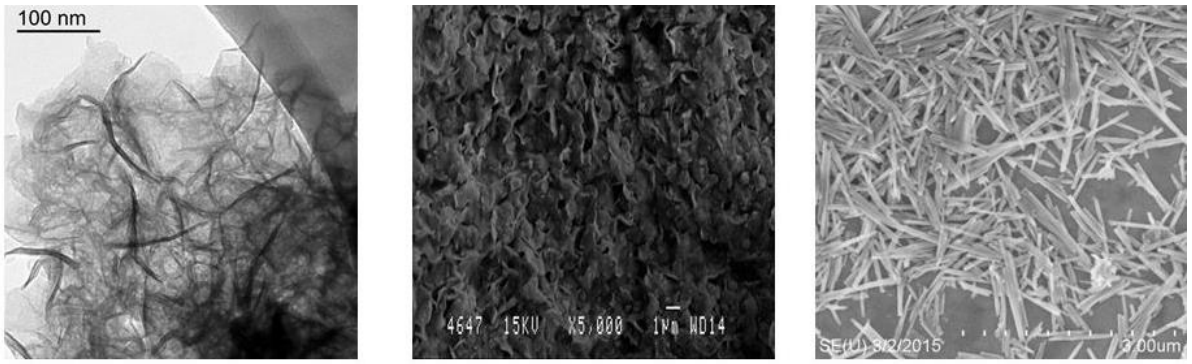

a b c

Figure 2. TEM, SEM images of exfoliated platy montmorillonite (a-b) and tubule halloysite (c).

Organic dye / inorganic clay composites can be obtained at room temperature from aqueous solutions dispersions using a wide range of pH[6]. The polarity of the clay sheet or fibers (often with SiO_2 surface) also stabilized many incorporated dyes. Surface modifiers, such as surfactants or silane coupling agents, can be used to adjust the nanoclay polarity [7]. These modifiers can open laminar structures and improve their exchange capacity. The benefits of the pH modification to modify the Al^{3+} site on the nanoclays were also reported[8]. The best synthetic or natural dyes – clay formulations which improved stability – needed maximal clay sheets exfoliation[9]. It takes a long time and essential energy for high stirring speed with smectite clays dispersion[10]. One has to avoid clay sheets aggregation which depends on the slurry ionic strength and the pH[11].

In the first approach with platy clays, a combination of the effect of surfactants, mordant salt and coupling agent (silane) to improve the organic dye – smectic nanoclay interactions were studied. A significant improvement of the organic dye incorporation into the lamellar dye structure was achieved with good color fastness[12].

In the second approach, we are developing dyes' loading into the inner lumens of tubule clay-halloysite. Halloysite clay has chemical structure similar to kaolin but is rolled in tubes[13]. Because of the tubule shape, halloysite does not stack together and can be easily exfoliated by steering. Halloysite clay is transparent and does not significantly change polymer composites'

transparency. Such core-shell dye-ceramic nanostructures look very promising for composite formations because the external surface of these loaded clay nanotubes is not modified with dye[14]. The loading of clay nanotube is produced by its few hours' exposure to saturated solution of a dye, then short rinsing to remove the outermost attached dye, and drying at 60-70 °C. After the lumen hydrophobization, oil-based dye may be also loaded into halloysite. The resulted colored clay powder may be tested for optical properties, dye stability and an extended time storage.

We describe perspectives of the formulations of hybrid pigments, using laminar and tubule nanoclays and examples of the encapsulated natural organic dyes. We demonstrated improvement of stability and optical properties of these organic-inorganic nanocomposites based on "green" chemical technology using natural often unstable dyes and natural clays, mostly platy montmorillonite or tubule halloysite.

2. Lamellar clays–dye pigmentation

Using statistical design of experiments, we combine additives in montmorillonite and hydrotalcite nanoclays in order to improve natural dyes stability. The hybrid pigments synthesis method was mechanical stirring using water/ethanol solutions with nanoclay dispersions, dyes and additives. Both lamellar clays were dispersed at 1,500 rpm for 24 h. Clay dispersions were prepared at 25 g/L in distilled water and ethanol (50/50), and pH was adjusted to 4-5 with HCl. The natural dyes solutions were perared using water solvent [$1 \cdot 10^{-03}$] M, and 0.27 ml/1ml of clay dispersion was added.

For the inner surface/ clay modification, we used first the surfactant, sodium dodecyl sulphate CAS: 151-21-3, $CH_3(CH_2)_{11}OSO_3Na$; the biomordant salt employed was the potassium alum $AlK(SO_4)_2 \cdot 12H_2O$, CAS 7784-24-9, and finally the coupling agent, or silane modifier, was the (3-aminopropyl)triethoxysilane $H_2N(CH_2)_3Si(OCH_3)_3$. We used the natural dyes extractions: beetroot red extract (NR), ($C_{24}H_{26}N_2O_{13}$), β-carotene (NO), ($C_{40}H_{56}$), copper

chlorophyll (NG), ($C_{34}H_{31}CuN4Na_3O_6$) and indigo carmine ($C1_6H_8N_2Na_2O_8S_2$). The powdered hybrid pigments were added to epoxy bioresin, improving their strength and stubility. With this we got colored nanocomposites that offer improved optical, mechanical and temperature properties, and also better UV-Vis light exposure color resistance. The color resistance after accelerated exposure in a climatic chamber was measured as the color difference ΔE_{ab}*. For instance, it was used a beetroot extraction, and the natural dye degradation (L9NR) was significantly higher than the degradation of the hybrid pigments obtained from laminar nanoclays in different synthesis conditions (Figure 3a).

The natural dyes degradation temperature was also increased (Figure 3b), and the dye migration was remarkably decreased under wet conditions. The standard scale obtained for all the hybrid pigments with different natural dyes (betanin, beta-carotene and chlorophyll) and laminar nanoclays was around 5[15]. The migration for each natural dye was avoided due to different laminar nanoclays (Figure 4a). Natural dyes incorporation as hybrid pigments using laminar nanoclays increase their industrial application possibilities[16].

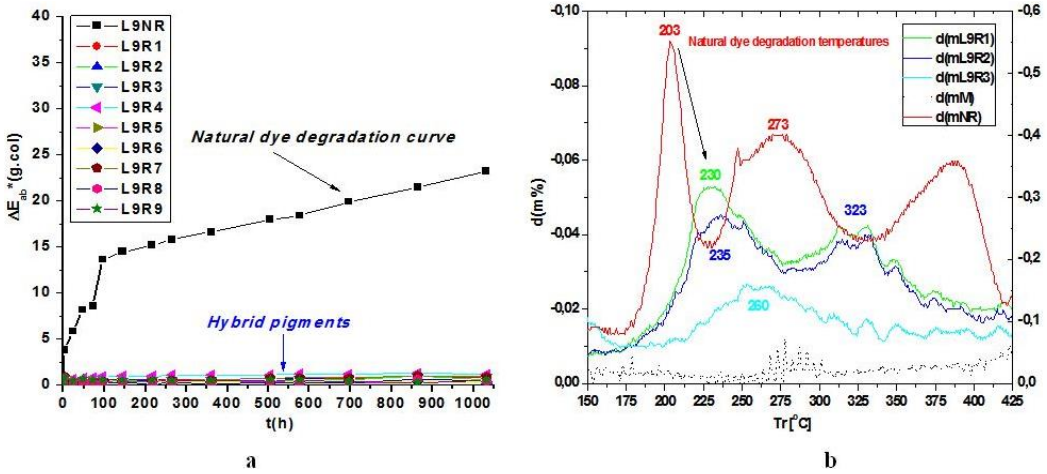

Figure 3. a) Color differences under accelerated UV-radiation test, for composite materials with epoxy bioresin and original beetroot extract (coded as L9NR) and hybrid pigments with laminar nanoclays under different synthesis conditions (L9R1-L9R9); b) First derivative of mass lost (%m) with temperature under oxidative conditions, with original beetroot extract (NR), montmorillonite clay (M), and hybrid pigments

Figure 4. a) Cotton standard fabrics after wet rub test, with composite materials using epoxy bioresin and natural chlorophyll extract (NG), and hybrid pigments with laminar nanoclays under different synthesis conditions. b) Hybrid pigments samples with indigo carmine and montmorillonite, or halloysite, or hydrotalcite nanoclay.

We then used synthetic dyes in halloysite pigmentation following the same synthesis process as was been used with lamellar nanoclays. We used the same modification process as with montmorillonite clay. However the surfactant and mordant effects were not relevant in the Indigo dye adsorption process. This could be because the clay-dye interaction is due to the ionic character of the Indigo Carmine. With nonionic dyes, the surface/lumen clay modification should be test, in order to improve the dye adsorption, and the clay-dye bonds. In this example we make comparisons using only Halloysite and Indigo Carmine, as first pure reference. As it is seen in the Figure 4b, the color intensity using the same dye concentration of indigo carmine was lower with halloysite nanotubes than using laminar hydrotalcite. However, the results with halloysite were better than the results with montmorillonite. It was impossible to introduce the indigo carmine into the montmorillonite structure, but both halloysite and hydrotalcite hybrids resulted in homogeneous pigments, with different hue and color appearances. Wet indigo pigment color is brighter than the dry one, because wetting of dispersed powder decreases the difference in refraction indices between material particles and the medium (in our case, ethanol instead of air), which in turn causes decrease of scattering by particles and allows percepting the more profound pigmentation (i.e., absorption). The degradation temperature curves for indigo carmine and the hybrid pigments with hydrotalcite

and halloysite demonstrated a significant thermal improvement: the main degradation peaks shifted from 441 °C for pure dye to 480 and 474 °C, respectively.

3. Halloysite nanotubes

Clay minerals have a layered structure of tetrahedral silica oxide and octahedral Al, Fe or Mg oxide. Kaolin clays are 1:1 phyllosilicates and montmorillonite clays are 2:1 phyllosilicates. Most of the research concerning clay materials is devoted to smectite clay group (such as montmorillonite, bentonite and hectorite) or kaolin where ca. 1 nm thick clay sheets are stacked in bulky platelets or processed with exfoliation to bilayer sheets. However, alumosilicate clays may have other morphologies, such as tubule halloysite and imogolite.

Halloysite is tubular clay ($Al_2Si_2O_5(OH)_4 \cdot nH_2O$, where n = 2-4) with diameter of 40-60 nm, inner lumen of 12-15 nm and length of ca. 1 μm which we pioneered for material composites research[14,21]. It is a natural biocompatible material available in thousands of tons at a low price which makes it a good candidate for nanoarchitectural dye composites. The inner lumen may be adjusted by etching to 20-30 % of the tube volume and loaded with dyes or other chemical agents, converting water soluble colors into polymer dispersable pigments[22]. *In vitro* and *in vivo* studies on biological cells, worms and small anymals indicate safety of halloysite, and it was tested for efficient mycotoxins adsorption in piglets' stomachs[14]. Halloysite is only a minor fraction of the clays used in industry; however, it has the advantage of utilizing inner tube lumen containers for dye loading. Besides, halloysite exfoliation is much easier because these clay nanotubes are not stacked together. Halloysite is stable until 500 °C when de-hydroxylation occurs with disruption of the tube wall's multilayer packing (X-ray peak at 0.72 nm disappears); however, the tubular shape of the clay is preserved up to 1100 °C[14]. Halloysites are the only available nanotubes with different outside (SiO_2) and

inside ($Al(OH)_3$) chemistry allowing for selective loading of negative dyes inside the tubes and positive molecules onto the outer surface.

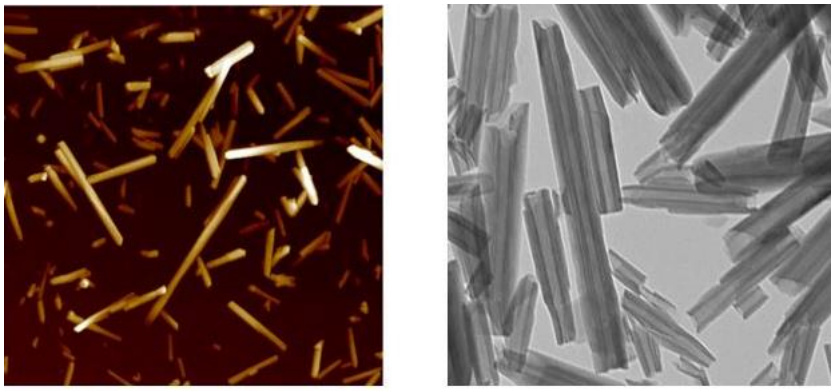

a b

Figure 5. AFM and TEM images of halloysite (a-b).

The outermost layer of halloysite is silica and innermost is alumina, so the tubes' ξ-potential derived by superposition of external SiO_2 negativity (of ca. -50 mV) and internal Al_2O_3 positivity (of ca. +20 mV) results in experimentally determined potential of ca. -30 mV at pH 4-8. This nanotube surface charge allows for moderate (for 2-3 hours) colloidal stability in water. Neutralization of inner positive charge with negative dyes allows increasing the aqueous colloidal stability of halloysite. In contrary, treatment of halloysite surface with cationic surfactant converts this system to compatible with nonpolar polymers.

For dye loading, its saturated solution in acetone, alcohol or water is mixed in excess amount with halloysite producing liquid slurry/paste. This is followed by 2-3 applications of for-vacuum for few minutes, until air is removed (visible bubbles) from the clay tubes and replaced by dye loading. Then, the sample may be rinsed with water to remove external dyes, and dried in oven. As a result, one can obtain homogeneously colored powder with long shelf-storage time. This fine powder may be added to color formulations or melted polymers. Halloysite itself is transparent, and addition of 5 wt % of pristine unloaded halloysite to 0.1 mm thick polyethylene films decreases its transparency by only a few percent.

4. Organic dyes-halloysite nanopigments

We utilized halloysite clay nanotubes for the adsorption of the indigo carmine and characterized its stability in pure and adsorbed forms. Dyes were loaded into the nanotubes at ca. 5 wt.% and the nanopigment temperature and pH stability was evaluated. The halloysite nanopigment had higher stability as compared to pure dye (Figure 7).

Indigo dye was dissolved in 1 mL of DI water under sonication; 40 mg of halloysite was added to this solution and sonicated to obtain a homogeneous solution. The mixture was placed in vacuum chamber for 3 cycles, 1 hour each, to ensure maximum loading. The samples were washed thoroughly with DI water 5 times by centrifuging at 10,621 rcf for 3 min. Washed samples were dried in a hot air oven at 60 °C. The dried powder was analyzed using thermogravimetric analysis to determine the loading efficiency. The procedure was repeated with different concentrations of dye to construct an empirical adsorption isotherm.

Figure 6. Halloysite-indigo carmine nanocomposites

Thermogravimetrical profiles studied individually for indigo carmine and halloysite indicated that the dye degrades at a temperature around 510 °C, which is not usual for organic compounds (Figure 7). This high degradation range is possibly due to the presence of sulphur in the structure of indigo carmine. The peak at 480-520 °C is characteristic of bare halloysite where there is a loss of hydroxyl groups at this temperature but does not degrade completely due to the presence of inorganic components. Peaks for both dye and halloysite can be seen in the TGA profile of halloysite-dye composites in the above temperature ranges. The amount of

dye in the composite was quantified as mass degraded over the given temperature range. Analysis of the profiles indicates 5.0 ± 0.5 wt.% dye loading efficiency.

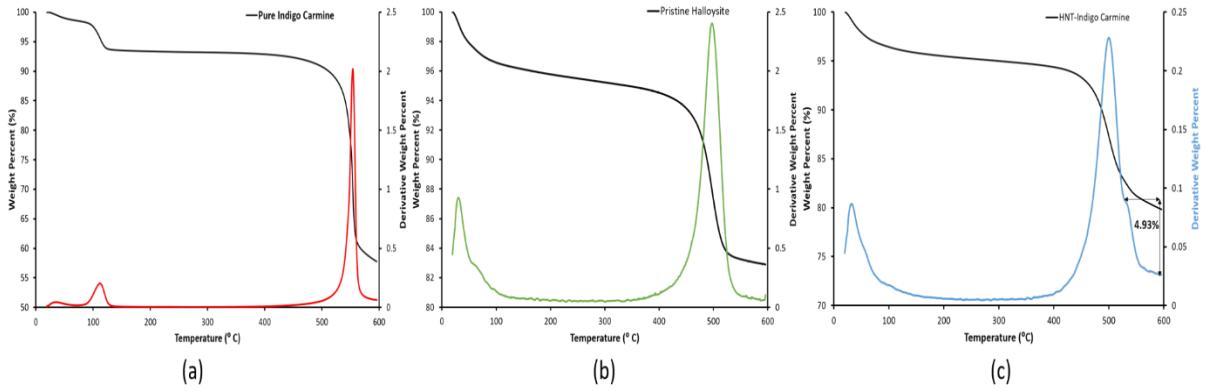

Figure 7. (a-c) Thermogravimetric profile of pristine halloysite, indigo carmine and composites.

Enhanced stability at high pH and temperature: Halloysite-indigo composites exhibit higher stability than pure dye at varying pH and temperature. As seen in Figure 8, even after overnight incubation in highly basic pH of 12, halloysite dye composites displayed greater stability. Similarly, greater temperature stability of dye loaded in halloysite was observed at high temperatures of 80 °C. This higher stability is due to the tubule core-shell nanopigment structure separating indigo from external conditions. Also, the adsorption process could have brought a structural change to indigo carmine imparting higher color stability. One can see a slight increase in the amount of dye in the case of halloysite composites.

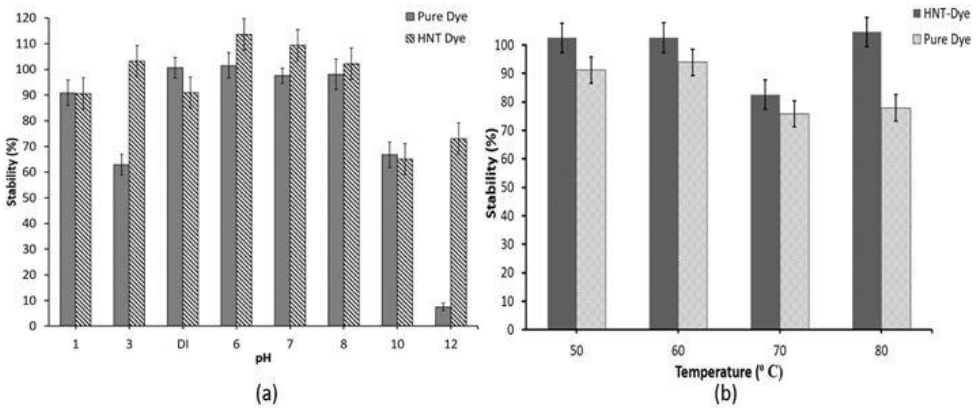

Figure 8. Stability of halloysite dye composites at varying pH (a) and temperature (b)

A synthetic pure dye rhodamine 6G, $C_{28}H_{31}ClN_2O_3$ was also used for halloysite nanopigments with the dye loading of 6 wt.%. Rhodmin loading capacity with halloysite was of about two

times higher than the one with kaolin. The only significant factors in the rhodamine adsorption into halloysite were the dye and mordant concentrations. Halloysite nanotubes adsorption capacity decreased with the ionic strength increment. At high dye concentration, it is better to have the lowest possible ionic strength.

Another example is loading water insoluble dye component of herbal natural color henna – lawsone. This colore formulation is widely used in hair care and is applied as aqeuos herbal slurry allowing to transfer this natural brown pigment to human hairs. To load lawsone, we first selectively hydrphobised halloysite lumens with anionc surfactant sodium dodecylesulfate and then loaded ca. 3 wt % of the dye from its aceton solution. Produced nanopigments allowed for safe and stable coloring with halloysite self-assembly onto hair surface.

5. Quantum dots / halloysite nanopigments

Luminescent quantum dots such as CdSe, CdTe, CdS, ZnS, In_2S_3, PbS nanocrystals and their hybrids structures are promising for pigments formulations and cellular labeling. Quantum dots are semiconductor particles with sizes of 1–10 nm and unique optical properties allowing for bright and stable coloring. They emit light with wavelength finely tuned from UV to IR depending on sizes, structure and composition. For example, CdSe provides visible mostly yellow radiation when particle size is 4-5 nm, the ZnS and ZnSe give ultraviolet light, and PbS, PbSe emit in the infrared region[19]. Quantum dots are used as labels for luminescence, fluorescence imaging, gas sensors, UV detectors, IR-detectors, and photovoltaic devices[19a]. It is a prospective class of biological labels with enhanced brightness, resistance to photo-bleaching, and multicolor light emissions that are not available with traditional organic dyes[20].

Though the fabrication of quantum dots can be based on different methods, the colloid synthesis is the most easily scalable. It is possible to produce safer quantum dots with blue to green spectral ranges using core-shell synthesis or rare earth metals such as neodymium instead of cadmium or

lead[21] to overcome the toxicity. Removal of heavy metals from quantum dots via phase interfacial reaction results in sulfur dots with low toxicity[22]. Typical quantum dots undergo the photo-induced oxidation and photoluminescence quenching in the presence of transition metal ions. Quantum dots are also stabilized with mercaptoacids and proteins[23]. For stabilization, quantum dots have been synthesized within various porous matrices – silica microtubes, mesoporous silica, and polymers[24].

To enhance stability and biocompatibility, we propose halloysite clay as a tubule nanotemplate for quantum dots synthesis. We employed two strategies: the quantum dots synthesis inside the clay nanotubes (Figure9 a-b) and their synthesis on the nanotube outer surface (Figure 9 c-d). We synthesized CdSe inside the lumens using two-step procedure: at first, we made a dispersion of halloysite in $Se(N_2H_4)$ solution of $Cd(NO_3)_2$ under ambient condition resulted in the chemicals loading into the tubes, and then we added $Se(N_2H_4)$ prepared from Se-powder and hydrazine hydrate results in the tube's loading. Then we added water solution of $Cd(NO_3)$ and stirred for one hour. As a result, the reaction propagated selectively through the tube's inner lumens. One can observe CdSe particles of 5-6 nm inside 15-nm diameter halloysite lumen (Figure 9 a-b). Some quantum dots are located near the lumen entrance, however, they may be washed out. An encasing of CdSe dots inside clay nanotubes allows the prevention of the semiconductor contact with exterior aqueous solutions, enhancing their stability and decreasing this core-shell system's toxicity. The powder of such clay encapsulated CdSe is bright red and being loaded in melted polyethylene or dispersed in water provides the stable color of dispersions.

In the second approach, we synthesized 3–4 nm diameter CdS and $Cd_xZn_{1-x}S$ nanodots on the outer tubes' surface (Figure 9, c-d). For this, Schiff bases were used as a ligand for metal complexes on the outer surface of halloysite. The blank experiments held without Schiff base linkage were not successful (the nanoparticles detached from halloysite and aggregated in bulk). When thioacetamide was used as sulfur precursor, the efficient CdS and $Cd_xZn_{1-x}S$

formation was observed in ethanol, with pH adjusted to 8 by aqueous ammonia. Similarly, ZnS, FeS and CuS, PbS nanodots were produced on the inner or outer halloysite surface.

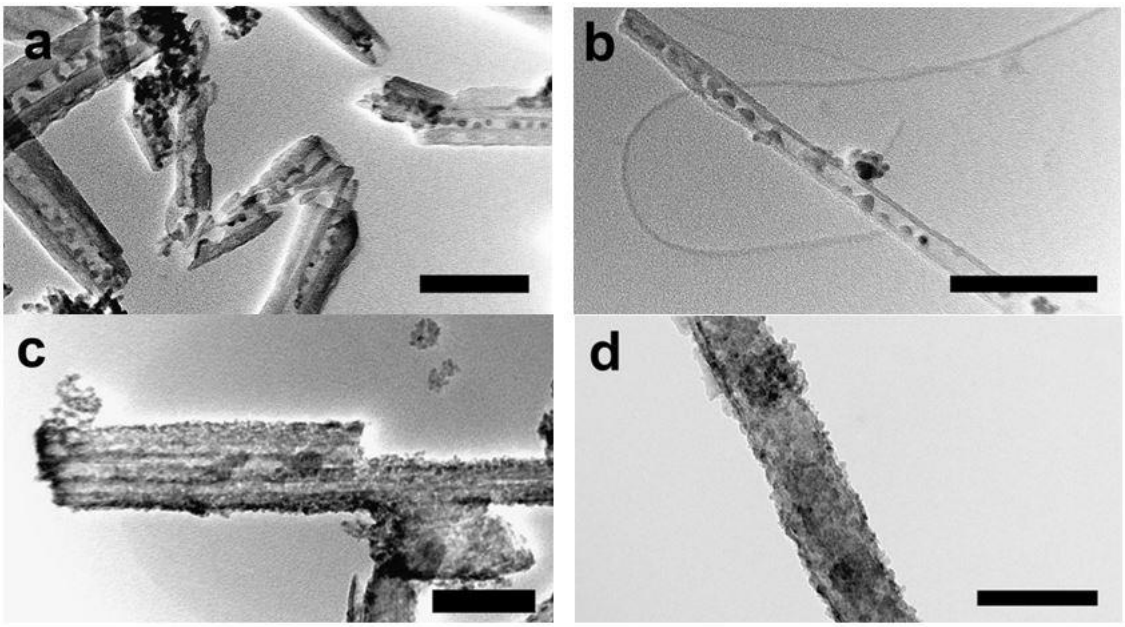

Figure 9. a-b) CdSe particles encased into halloysite lumen; c) CdS and d) $Cd_xZn_{1-x}S$ particles onto the tubes' surface. Bars, 100 nm.

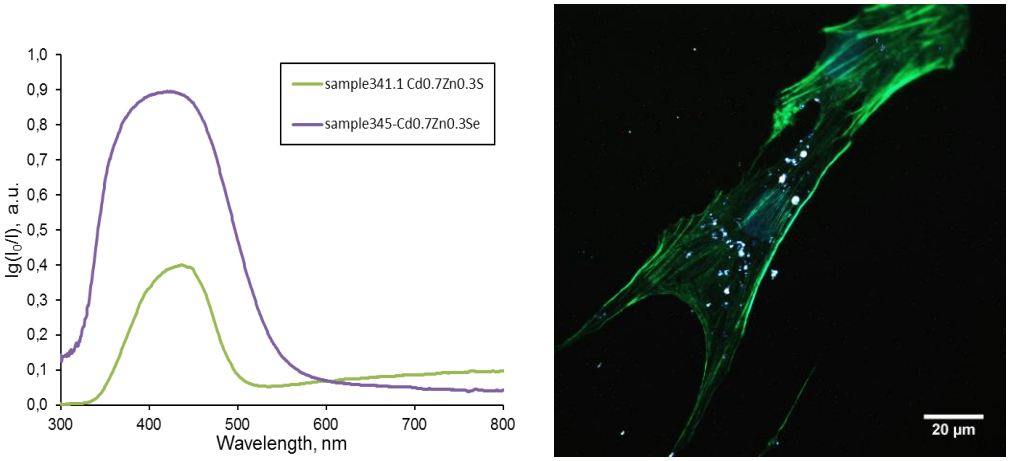

a b

Figure 10. a) Reflectance spectra of CdS, CdSe and $Cd_xZn_{1-x}S$ halloysite-nanodots. b) Merged dark-field\fluorescence micrograph of human skin fibroblast cell, nucleus stained with DAPI (blue), actin filaments stained Falloidin-AF488 (green), and CdS quantum dots loaded halloysite (white spots).

To investigate the uptake / labelling and potential toxicity of quantum dots loaded halloysite we have employed an in vitro toxicity model based on human primary and cancer cell cultures. We have used human skin fibroblasts and human prostate cancer cells[25]. Figs. 10-11 show that quantum dots loaded halloysite are clearly seen as bright dots inside the skin fibroblast

cells. The indication of low toxicity of quantum dots loaded halloysite is the preserved growth rate of human cells incubated in media supplemented with the quantum dots loaded halloysite. Depending on the chemical modification, quantum dots loaded halloysite are either diffusely distributed within the cytoplasm or predominantly agglomerated in perinuclear region (Figure 11), suggesting that a certain mechanism of controllable delivery might be employed.

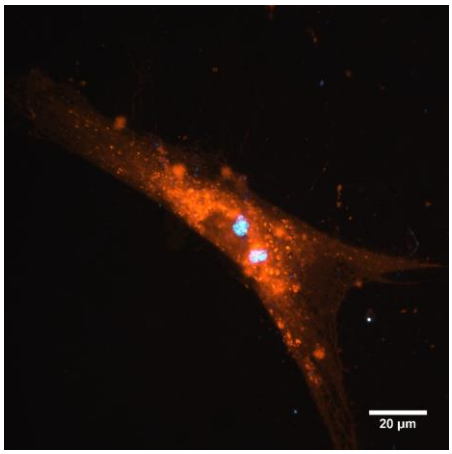

Figure 11. Merged dark-field and fluorescence images of human skin fibroblasts after taking up $Cd_xZn_{x-1}S$ quantum dots loaded halloysite (seen as bright agglomerated spots around nucleus region). The cellular membranes were stained with DiL membrane tracker for better contrast.

More importantly, the uptake of quantum dots loaded halloysite does not apparently disrupt the internal membrane-enclosed organelles, as demonstrated by corresponding DiL-stained fluorescence images of the same regions. The similar results were obtained with PC3 cells. Taking advantage of the intrinsic fluorescence properties of quantum dots arrested within halloysite, we have also imaged them using laser scanning confocal microscopy. As shown in Figure 12, the quantum dots loaded halloysite can be easily detected inside the cytoplasm of DiL-labelled human skin fibroblasts.

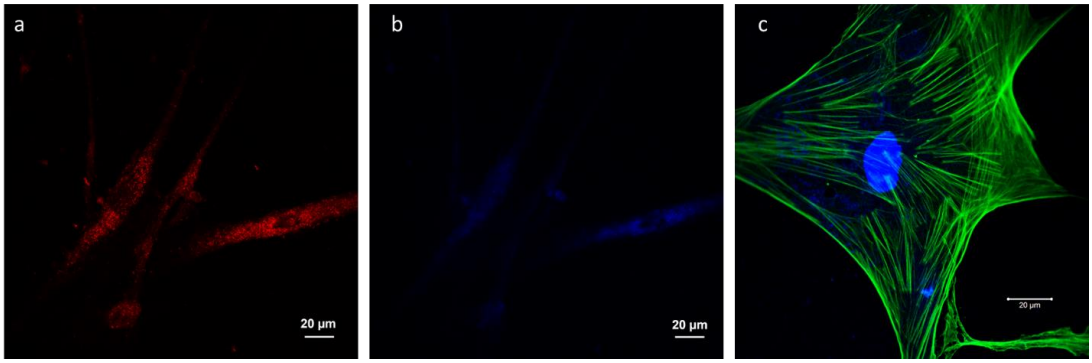

Figure 12. Laser scanning confocal images of human skin fibroblasts cells incubated with $Cd_xZn_{x-1}S$ quantum dots loaded halloysite. The cells were counter-stained with DiL (a) and FITC-labelled phalloidin and DAPI (c) to visualize cellular membranes, cytoskeleton actin filaments and nuclei (note a large aggregate of quantum dots loaded halloysite in a lower right part of the cells, other particles are diffusely located within the cytoplasm).

We have also investigated the cytoskeleton formation in cells incubated with quantum dots loaded halloysite cells. As shown in Figure 12 c, the micro-organization of actin filaments was not disrupted by quantum dots loaded halloysite, which also indicates its high biocompatibility. The labelling of human cells with halloysite – quantum dots demonstrated the similar behavior and low toxicity as pristine (empty) nanotubes[26]. Ideally, the use of quantum dots loaded halloysite would allow for the efficient fluorescent labelling of human cells and find applications in cell-based therapies and tissue engineering.

6. Conclusions

We describe a stategy for formulations of hybrid pigments, using laminar, tubule and fiber nanoclays and industrial natural dyes. The optical, thermal and fastness improvements of organic dyes with their laminar / tubular nanoclays interactions were demonstrated. Using platy montmorillonite or tubule halloysite it is possible to enhance the stability of natural dyes and convert them from water soluble to pigments encasing dyes in ceramic nanocontainers. A possibility of selective external or internal dye adsorption to nanoclay allows for varying dye loading from 10-20 wt % for nanotubes' lumens, to 10-30 wt % for platy multilamellar clays.

The synthesis of a novel class of core-shell nanostructures - quantum dots arrested within halloysite lumens, opens the avenues for biocompatible and efficient labelling of human cells, which may find numerous applications in cellular-based therapies and tissue engineering for tracking of target cells. We confirmed that halloysite acts as a biosafe and non-toxic envelope to enclose fluorescent quantum dots within light-scattering nanoclay tubes. This allows for fabricating nanosized beacons with double functionality for both fluorescent and dark-field imaging within live human cells.

Funding sources:

YL, VV, AS, and AN thank the Ministry of Education and Science of the Russian Federation (grant 14.Z50.31.0035) for funding this work.

Acknowledgements:

Authors are grateful to Mikhail S. Kotelev (Gubkin University) for the TEM micrographs. The biocell labelling work was performed by RF and ER according to the Russian Government Program of Competitive Growth of Kazan Federal University. Also we thank the Spanish Ministry of Economy and Competitiveness for funding Projects DPI2011-30090-C02-02 and DPI2015-68514-R.

Received: ((will be filled in by the editorial staff))
Revised: ((will be filled in by the editorial staff))
Published online: ((will be filled in by the editorial staff))

References

[1] a) Technical guidance document CR-48-96-001-EN-C, European Comission, **1996**. b) A. Massos, A. Turner, *Environ. Pollut.* **2017**, *227*, 139.

[2] a) M. Mirjalili, K. Nazarpoor, L. Karimi, *Journal of Cleaner Production* **2011**, *19*, 1045. b) I. Ebrahimi, M. Parvinzadeh Gashti, *Color. Technol.* **2016**, *132*, 162.

[3] L. J. Rather, I. Shahid ul, M. Shabbir, M. N. Bukhari, M. Shahid, M. A. Khan, F. Mohammad, *Journal of Environmental Chemical Engineering* **2016**, *4*, 3041.

[4] L. A. Polette-Niewold, F. S. Manciu, B. Torres, M. Alvarado Jr, R. R. Chianelli, *Journal of Inorganic Biochemistry* **2007**, *101*, 1958.

[5] Y. Kohno, M. Inagawa, S. Ikoma, M. Shibata, R. Matsushima, C. Fukuhara, Y. Tomita, Y. Maeda, K. Kobayashi, *Applied Clay Science* **2011**, *54*, 202.

[6] E. Baena-Murillo, B. Micó-Vicent, F.M. Martínez-Verdú, 2013.

[7] M. Huskić, M. Žigon, M. Ivanković, *Applied Clay Science* **2013**, *85*, 109.

[8] Y. Kohno, S. Asai, M. Shibata, C. Fukuhara, Y. Maeda, Y. Tomita, K. Kobayashi, *J. Phys. Chem. Solids* **2014**, *75*, 945.

[9] Y. Kohno, E. Haga, K. Yoda, M. Shibata, C. Fukuhara, Y. Tomita, Y. Maeda, K. Kobayashi, *J. Phys. Chem. Solids* **2014**, *75*, 48.

[10] a) C.-C. Wang, L.-C. Juang, T.-C. Hsu, C.-K. Lee, J.-F. Lee, F.-C. Huang, *J. Colloid Interface Sci.* **2004**, *273*, 80. b) H. Salam, Y. Dong, I. Davies, in *Fillers and Reinforcements for Advanced Nanocomposites*, Woodhead Publishing **2015**, p. 101-112.

[11] a) E. Tombacz, M. Szekeres, *Appl. Clay Sci.* **2004**, *27*, 75; b) [1] J. D. G. Duran, M. M. Ramos-Tejada, F. J. Arroyo, F. Gonzalez-Caballero, *J. Colloid Interface Sci.* **2000**, *229*, 107.

[12] B. Micó-Vicent, Martínez-Verdú, F.M. Spain Patent ES2568833, 2017.

[13] a) Y. Lvov, W. Wang, L. Zhang, R. Fakhrullin, *Adv. Mater.* **2016**, *28*, 1227, b) M. Liu, Z. Jia, D. Jia, C. Zhou, *Prog. Polym. Sci.* **2014**, *39*, 1498; c) M. Du, B. Guo, D. Jia, *Polym. Int.* **2010**, *59*, 574.

[14] a) P. Yuan, D. Tan, F. Annabi-Bergaya, *Appl. Clay Sci.* **2015**, *112–113*, 75. b) G. Cavallaro, G. Lazzara, S. Milioto, *J. Phys. Chem. C* **2012**, *116*, 21932.

[15] E.ISO, EN ISO 2001, 105.

[16] B. Micó-Vicent, J. Jordán, F. Martínez-Verdú, R. Balart, *J. Mater. Sci.* **2017**, *52*, 889.

[17] R. R. Price, B. P. Gaber, Y. Lvov, *J. Microencapsul.* **2001**, *18*, 713.

[18] a) E. Joussein, S. Petit, J. Churchman, B. Theng, D. Righi, B. Delvaux, *Clay Miner.* **2005**, *40*, 383. b) Y. M. Lvov, D. G. Shchukin, H. Mohwald, R. R. Price, *ACS Nano* **2008**, *2*, 814. c) M. Du, B. Guo, D. Jia, *Polym. Int.* **2010**, *59*, 574. d) Y. Lvov, E. Abdullayev, *Prog. Polym. Sci.* **2013**, *38*, 1690. e) M. Liu, Z. Jia, D. Jia, C. Zhou, *Prog. Polym. Sci.* **2014**, *39*, 1498. f) E. Abdullayev, A. Joshi, W. Wei, Y. Zhao, Y. Lvov, *ACS Nano* **2012**, *6*, 7216. g) W. O. Yah, A. Takahara, Y. M. Lvov, *J. Am. Chem. Soc.* **2012**, *134*, 1853. h) G. Cavallaro, G. Lazzara, S. Milioto, F. Parisi, V. Sanzillo, *ACS Appl. Mater. Interfaces* **2014**, *6*, 606.

[19] a) S. Silvi, A. Credi, *Chem. Soc. Rev.* **2015**, *44*, 4275. b) T. Jin, Y. Imamura, *ECS J. Solid State Sci. Technol.* **2016**, *5*, R3138. c) Z. Xu, J. Yan, C. Xu, C. Cheng, C. Jiang, X. Liu, J. Qiu, *J. Alloys Compd.* **2017**, *711*, 58.

[20] E. Petryayeva, W. R. Algar, I. L. Medintz, *Appl. Spectrosc.* **2013**, *67*, 215.

[21] a) H. Shen, X. Bai, A. Wang, H. Wang, L. Qian, Y. Yang, A. Titov, J. Hyvonen, Y. Zheng, L. S. Li, *Adv. Funct. Mater.* **2014**, *24*, 2367. b) Q. Li, X. Jin, Y. Yang, H. Wang, H. Xu, Y. Cheng, T. Wei, Y. Qin, X. Luo, W. Sun, S. Luo, *Adv. Funct. Mater.* **2016**, *26*, 254.

[22] S. Li, D. Chen, F. Zheng, H. Zhou, S. Jiang, Y. Wu, *Adv. Funct. Mater.* **2014**, *24*, 7133.

[23] a) A. Benayas, F. Ren, E. Carrasco, V. Marzal, B. Del Rosal, B. A. Gonfa, Á. Juarranz, F. Sanz-Rodríguez, D. Jaque, J. García-Solé, D. Ma, F. Vetrone, *Adv. Funct. Mater.* **2015**, *25*, 6650. b) J. Chen, Y. Kong, W. Wang, H. Fang, Y. Wo, D. Zhou, Z. Wu, Y. Li, S. Chen, *Chem. Commun.* **2016**, *52*, 4025.

[24] a) V. Malgras, S. Tominaka, J. W. Ryan, J. Henzie, T. Takei, K. Ohara, Y. Yamauchi, *J. Am. Chem. Soc.* **2016**, *138*, 13874. b) A. Tiwari, S. J. Dhoble, *RSC Adv.* **2016**, *6*, 64400.

[25] a) M. R. Dzamukova, E. A. Naumenko, E. V. Rozhina, A. A. Trifonov, R. F. Fakhrullin, *Nano Res.* **2015**, *8*, 2515. b) S. Tai, Y. Sun, J. M. Squires, H. Zhang, W. K. Oh, C.-Z. Liang, J. Huang, *Prostate* **2011**, *71*, 1668.

[26] a) S. A. Konnova, I. R. Sharipova, T. A. Demina, Y. N. Osin, D. R. Yarullina, O. N. Ilinskaya, Y. M. Lvov, R. F. Fakhrullin, *Chem. Commun.* **2013**, *49*, 4208. b) G. I. Fakhrullina, F. S. Akhatova, Y. M. Lvov, R. F. Fakhrullin, *Environ. Sci. Nano* **2015**, *2*, 54. c) M. Kryuchkova, A. Danilushkina, Y. Lvov, R. Fakhrullin, *Environ. Sci. Nano* **2016**, *3*, 442.

Author biographies

Bàrbara Micó Vicent, is a Professor of statistics at the Polytechnic University of Valencia and a researcher in the Colour & Vision Group at the University of Alicante, Spain. She is an expert in color science and industrial technologies, focused on the development of hybrid pigments and the advanced multivariate statistical applications in dye formulations.

Vladimir Vinokurov is Professor and Chair of Physical and Colloidal Chemistry at I.Gubkin Russian State University of Oil & Gas. He pioneered a number of colloidal formulations for oil drilling technologies and advanced catalysis protected with 27 Russian patents and published over 190 peer reviewed papers on organic-inorganic nano/micro composites.

Rawil Fakhrullin is a head of Bionanotechonlogy laboratory, Institute of Fundamental Medicine and Biology, Kazan Federal University, Republic of Tatarstan. He received his PhD from Kazan State University in 2006. He has worked as a visiting scientist in University of Hull (UK), Yeditepe University (Turkey) and Louisiana Tech University (USA). In 2016, he has been a visiting professor at University of Palermo, Italy. His research is focused on cell-surface engineering, drug delivery, tissue engineering and nanotoxicity. He has published 65 papers, 6 book chapters and edited two books on cell-surface engineering and clay-polymer composites.

Yuri M. Lvov is a Professor of Chemistry, T. Pipes Eminent Endowed Chair on Micro and Nanosystems at Louisiana Tech University. He got Ph.D. from M.Lomonosov Moscow State University and then worked in Max Planck Institute for Colloids and Interfaces, Germany, in Japan (NIMS, Tsukuba), and at the Naval Research Laboratory, USA. His area of interest is nanoassembly of ultrathin organized films, construction of ordered shells on tiny templates (drug nanocapsules), clay nanotubes for controlled release of chemical agents and drugs, functional organic-inorganic nanocomposites. He published 250 papers and has over 22,000 citations of his works.